Supporting Material

Design of highly conductive iongel soft solid electrolytes for Li-O_2 batteries

Marta Alvarez-Tirado[1,2,4], Laurent Castro[2], Gregorio Guzmán-González[1,5], Aurélie Guéguen[2], Liliana C. Tomé[1,6], David Mecerreyes[1,3,*]

[1]POLYMAT University of the Basque Country UPV/EHU, Donostia-San Sebastian 20018, Spain.

[2]Toyota Motor Europe Research & Development 1, Advanced Material Research, Battery & Fuel Cell, Zaventem B-1930, Belgium.

[3]Ikerbasque, Basque Foundation for Science, Bilbao E-48011, Spain.

[4]Present address: CIDETEC, Basque Research and Technology Alliance (BRTA), Donostia-San Sebastián 20014, Spain.

[5]Present address: Departamento de Química, Universidad Autónoma Metropolitana-Iztapalapa, México City 09340, México.

[6]Present address: LAQV-REQUIMTE, Department of Chemistry, NOVA School of Science and Technology, FCT NOVA, Universidade NOVA de Lisboa, 2829-516 Caparica, Portugal.

***Correspondence to:** Dr. David Mecerreyes, POLYMAT University of the Basque Country UPV/EHU, Joxe Mari Korta Building, Avenida Tolosa 72, Donostia-San Sebastian 20018, Spain. E-mail: david.mecerreyes@ehu.eus

EXPERIMENTAL

Materials

N,N-diethyl-N-methyl-N-(2-methoxyethyl)ammonium bis(trifluoromethanesulfonyl)imide (DEME-TFSI, Solvionic, 99.9%), poly(ethylene glycol) dimethacrylate (PEGDM, Aldrich, Mn 550) and 2-hydroxy-2-methylpropiophone (DAROCUR, Aldrich, 97%) were dried by adding activated 4 Å molecular sieves (Aldrich, 4–8 mesh) for 5 d. Additionally, materials were dried under vacuum for 24 h at room temperature (RT) before introducing them into an argon-filled glovebox. The water content was measured by Coulometric Karl Fischer titration and decreased to 17.9 ± 4.6 ppm for PEGDM and 10.8 ± 0.6 ppm for DEME-TFSI. N,N-diethyl-N-methyl-N-((trifluoroethoxy) ethyl) ammonium bis(trifluoro methylsulfonyl)imide (labeled as FD-TFSI in the manuscript) was previously synthesized by Solvionic in a previous work[1]. The ionic liquid was kept in the glovebox with the activated 4 Å molecular sieves (Aldrich, 4–8 mesh).

Lithium bis(trifluoromethanesulfonyl)imide (LiTFSI, IoLiTec, 99.0%), lithium bis(fluorosulfonyl)imide (LiFSI, TCI, >98.0% (T)), lithium bis(perfluoroethylsulfonyl)imide (LiBETI, IoLiTec, battery grade) and lithium nanofluoro-1-butanesulfonate ($LiC_3F_9SO_3$, TCI, >95.0%) were vacuum dried at 100 ℃ for 24 h before use for electrolyte preparation. LiFSI was vacuum dried at 50 ℃ for 48 h before use for electrolyte preparation. N,N-diethyl-N-methyl-N-(2-methoxyethyl)ammonium bromide (DEME-Br, Solvionic, 98%) and the salts used for the ionic liquid synthesis were used as received.

All material preparation and cells assemblies were carried out inside an argon-filled glovebox with levels of H_2O < 0.01 ppm and O_2 < 0.01 ppm.

Synthesis of ionic liquids

The $[TFSI]^-$ anion of the DEME-TFSI ionic liquid was replaced by different anions, namely, bis(fluorosulfonyl)imide [FSI]-, bis(perfluoroethylsulfonyl)imide [BETI]- and nanofluoro-1-butanesulfonate $[C_3F_9SO_3]$-. Hence, four ionic liquids labeled as DEME-TFSI, DEME-FSI, DEME-BETI and DEME-$C_3F_9SO_3$ were synthesized by a salt metathesis reaction, similar to that previously reported in the literature[1–3]. As shown in Scheme 1, an anion exchange reaction occurred between a Br^- anion (from DEME-Br) and the negative ion of a commercially available monovalent salt (e.g., $X^+ = Na^+$, Li^+ or K^+) containing the Y^- of interest (e.g., $Y^- = TFSI^-$, $BETI^-$ or $C_3F_9SO_3^-$).

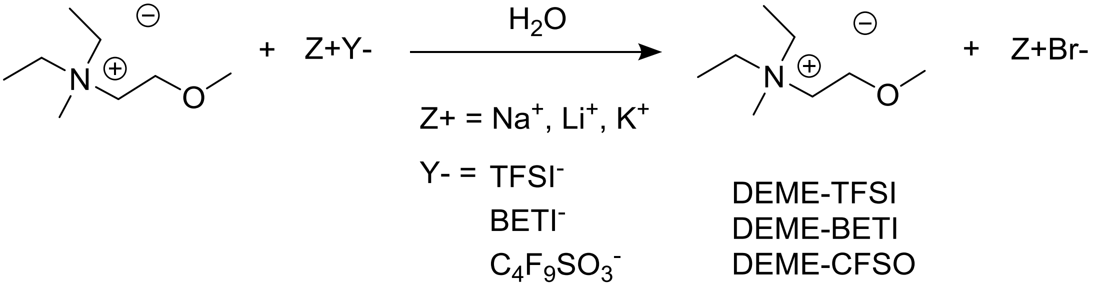

Scheme 1. Ionic liquid synthesis scheme.

N,N-diethyl-N-methyl-N-(2-methoxyethyl)ammonium bis(trifluoromethanesulfonyl)imide (DEME-TFSI)

26 mmol of LiTFSI were dissolved in 50 mL of distilled water at RT and added dropwise to an aqueous solution of 20 mmol of DEME-Br dissolved in 20 mL of distilled water at RT. The mixtures were stirred overnight. The ionic liquid was then extracted with dichloromethane (3×40 mL) and washed with distilled water (2±10 mL). The mixture was then vacuum dried at 60 ℃ for 2 h to evaporate the solvents and vacuum dried for another 2 h before introducing the resulting transparent ionic liquid to an argon-filled glovebox. The water content was 130.77 ± 5.6 ppm, as measured by Coulometric Karl Fischer titration. Yield: 7.09 g (98.06%). Found: ^{1}H NMR (400 MHz, DMSO-d6): δ (ppm) = 3.71 (broad s, 2H, $-CH_2-CH_2-O-$), 3.45 (t, 2H, $-CH_2-CH_2-O-$), 3.34 (c, 8H, $-N-CH_2-CH_3$), 3.29 (s, 2H, $-N-CH_3$), 2.95 (s, 3H, $-O-CH_3$), 1.20 (t, 6H, $-N-CH_2-CH_3$). ^{13}C NMR (101 MHz, DMSO-d6): δ (ppm) = 124.26 ($-CF_3$), 121.07 ($-CF_3$), 117.87 ($-CF_3$), 114.67 ($-CF_3$), 65.16 (s, $-CH_2-CH_2-O-$), 59.12 (s, $-CH_2-CH_2-O-$), 58.19 (s, $-O-CH_3$), 56.32 (s, $-N-CH_2-CH_3$), 47.16 (s, $-N-CH_3$), 7.53 (s, $-N-CH_2-CH_3$). ^{19}F NMR (376 MHz, DMSO-d6): δ (ppm) = -78.75 (s, $-CF_3$).

N,N-diethyl-N-methyl-N-(2-methoxyethyl)ammonium bis(fluorosulfonyl)imide (DEME-FSI)

The procedure previously described for DEME-TFSI was also used for the synthesis of DEME-FSI. LiFSI salt was used instead and a transparent ionic liquid was obtained after drying. The water content was 162.93 ± 7.3 ppm, as measured by Coulometric Karl Fischer titration. Yield: 6.49 g (97.62%). Found: ^{1}H NMR (400 MHz, DMSO-d6): δ (ppm) = 3.71 (broad s, 2H, $-CH_2-CH_2-O-$), 3.45 (t, 2H, $-CH_2-CH_2-O-$), 3.34 (c, 8H, $-N-CH_2-CH_3$), 3.29 (s, 2H, $-N-CH_3$), 2.95 (s, 3H, $-O-CH_3$), 1.21 (t, 6H, $-N-CH_2-CH_3$). ^{13}C NMR (101 MHz, DMSO-d6): δ (ppm) = 65.19 (s, $-CH_2-CH_2-O-$), 59.18 (s, $-CH_2-CH_2-O-$), 58.22 (s, $-O-CH_3$), 56.38 (s, $-N-CH_2-CH_3$), 47.19 (s, $-N-CH_3$), 7.55 (s, $-N-CH_2-CH_3$).^{19}F NMR (376 MHz, DMSO-d6): δ (ppm) = -51.6 (s, -F).

N,N-diethyl-N-methyl-N-(2-methoxyethyl)ammonium bis(perfluoroethylsulfonyl)imide (DEME-BETI)

The procedure previously described for DEME-TFSI was also used for the synthesis of DEME-BETI. LiBETI salt was used instead and a viscous transparent ionic liquid was obtained after drying. The water content was 98.93 ± 9.0 ppm, as measured by

Coulometric Karl Fischer titration. Yield: 10.56 g (99.04%). Found: ^{1}H NMR (400 MHz, DMSO-d6, Figure S2a): δ (ppm) = 3.71 (broad s, 2H, -CH$_2$-CH$_2$-O-), 3.45 (t, 2H, -CH$_2$-CH$_2$-O-), 3.34 (c, 8H, -N-CH$_2$-CH$_3$), 3.29 (s, 2H, -N-CH$_3$), 2.95 (s, 3H, -O-CH$_3$), 1.20 (t, 6H, -N-CH$_2$-CH$_3$). ^{13}C NMR (101 MHz, DMSO-d6, Figure S2b): δ (ppm) = 119.20 (-CF$_2$-CF$_3$), 116.34 (-CF$_2$-CF$_3$), 114.22 (-CF$_2$-CF$_3$), 113.85 (-CF$_2$-CF$_3$), 111.30 (-CF$_2$-CF$_3$), 110.93 (-CF$_2$-CF$_3$), 65.19 (s, -CH$_2$-CH$_2$-O-), 59.14 (s, -CH$_2$-CH$_2$-O-), 58.23 (s, -O-CH$_3$), 56.33 (s, -N-CH$_2$-CH$_3$), 47.18 (s, -N-CH$_3$), 7.57 (s, -N-CH$_2$-CH$_3$). ^{19}F NMR (376 MHz, DMSO-d6, Figure S2c): δ (ppm) = -78.54 (s, -CF$_2$-CF$_3$); -117.41 (s, -CF$_2$-CF$_3$).

N,N-diethyl-N-methyl-N-(2-methoxyethyl)ammonium nonafluoro-1-butanesulfonate (DEME-$C_3F_9SO_3$)

26 mmol of KC$_3$F$_9$SO$_3$ were dissolved in 100 mL of distilled water at 60 ℃ and added dropwise to an aqueous solution of 20 mmol of DEME-Br dissolved in 20 mL of distilled water at 50 ℃ in an oil bath. The mixtures were stirred overnight at 40 ℃. The ionic liquid was then extracted with dichloromethane (5×40 mL) and washed with distilled water (3×10 mL). The mixture was then vacuum dried at 80 ℃ for 2 h to evaporate the solvents and vacuum dried for another 2 h before introducing the resulting transparent ionic liquid to an argon-filled glovebox. The water content was 259.10 ± 7.3 ppm, as measured by Coulometric Karl Fischer titration. Yield: 8.80 g (96.09%). Found: ^{1}H NMR (400 MHz, acetone-d6): δ (ppm) = 3.71 (broad s, 2H, -CH$_2$-CH$_2$-O-), 3.45 (t, 2H, -CH$_2$-CH$_2$-O-), 3.34 (c, 8H, -N-CH$_2$-CH$_3$), 3.29 (s, 2H, -N-CH$_3$), 2.95 (s, 3H, -O-CH$_3$), 1.20 (t, 6H, -N-CH$_2$-CH$_3$). ^{13}C NMR (101 MHz, DMSO-d6): δ (ppm) = 119.05 (q, -CF$_2$-CF$_3$), 116.05 (q, -CF$_2$-CF$_3$), 113.52 (d, -CF$_2$-CF$_3$), 110.98 (q, -CF$_2$-CF$_3$), 108.38 (q, -CF$_2$-CF$_3$), 65.19 (s, -CH$_2$-CH$_2$-O-), 59.14 (s, -CH$_2$-CH$_2$-O-), 58.23 (s, -O-CH$_3$), 56.33 (s, -N-CH$_2$-CH$_3$), 47.18 (s, -N-CH$_3$), 7.57 (s, -N-CH$_2$-CH$_3$). ^{19}F NMR (376 MHz, acetone-d6): δ (ppm) = -80.87 (s, -CF$_2$-CF$_2$-CF$_2$-CF$_3$), -115.33 (s, -CF$_2$-CF$_2$-CF$_2$-CF$_3$), -121.89 (s, -CF$_2$-CF$_2$-CF$_2$-CF$_3$), -126.20 (s, -CF$_2$-CF$_2$-CF$_2$-CF$_3$).

Electrolyte preparation

Ionic liquid electrolytes (ILEs). LiTFSI was mixed with DEME-FSI and DEME-TFSI at a concentration of 20 mol.% and stirred for 2 h at RT. LiTFSI was mixed with FD-TFSI, DEME-BETI and DEME-$C_3F_9SO_3$ at 20 mol.% and stirred for 4, 4 and 6 h at 50 ℃, respectively. LiFSI was mixed with DEME-FSI at 20 mol.% for 2 h at RT. LiBETI was mixed with DEME-BETI at 20 mol.% for 8 h at 50 ℃. $LiC_3F_9SO_3$ was mixed with DEME-$C_3F_9SO_3$ at 20 mol.% for 18 h at 60 ℃.

Iongel electrolytes. The ILE mixtures were mixed with the crosslinker (PEGDM) at a ratio of 90:10 wt.% for the ILE and crosslinker, respectively (Table S1). The mixtures were stirred for 2 h at 50 ℃ (1 h at RT for DEME-FSI- and DEME-TFSI-based electrolytes) before adding a DAROCUR photoinitiator at 3% w/w of monomers. The iongels were obtained by drop casting the pre-warmed mixture on a silicon mold (Φ 11.28 mm circular voids) and irradiating with a UV-LED lamp for <2 min (300–400 nm with a peak at 385 nm, Lightningcure® V3, Hamamatsu).

In addition, liquid electrolyte mixtures based on FD-TFSI were mixed with the crosslinker (PEGDM) at different ratios for impedance measurements (Table S1). The mixtures were stirred for at least 2 h at 50 ℃ before adding the DAROCUR photoinitiator at 3% w/w of monomers. The iongels were also obtained by drop casting.

Table S1. Iongel electrolyte compositions in wt.% based on FD-TFSI ionic liquid.

Sample	Liquid electrolyte[a]	PEGDM[b]
Iongel-FD-80	80	20
Iongel-FD-85	85	15
Iongel-FD-90	90	10

[a]20 mol.% of LiTFSI in FD-DEME; [b]Poly(ethylene glycol) dimethacrylate.

Materials characterization

Ionic liquids. The chemical characterization was carried out using Fourier transform infrared (FTIR) spectroscopy with attenuated total reflectance with a Bruker Alpha l spectrometer. The measuring probe was at RT and under an air atmosphere. ^1H, ^{13}C and

^{19}F nuclear magnetic resonance (NMR) spectra (Bruker Avance III 400 MHz Digital NMR spectrometer) were also used to provide chemical structural information. Differential scanning calorimetry (DSC) thermograms were undertaken using a Perkin Elmer 8500 DSC equipped with an Intracooler III and calibrated with indium and tin standards. Samples were first heated with a scan rate of 10 ℃ min^{-1} from RT to 150 ℃ and held for 10 min to erase thermal history, followed by cooling to –80 ℃ and heating until 200 ℃. Both non-isothermal scans were recorded at ± 10 ℃ min^{-1}. Dynamic viscosity was undertaken using an Antor Paar rheometer at a constant 200 s^{-1} shear rate and using a 40 mm steel 2 ° cone at both 25 and 60 ℃.

Iongels. Thermal gravimetric analysis (TGA) employing a TGA Q 500 (TA instruments) was undertaken to investigate the thermal stability of the iongels. The samples were heated from RT to 600 ℃ at a heating rate of 10 ℃ min^{-1} under a nitrogen flux of 90 mL/min.

The mechanical properties of the iongels were studied by dynamic mechanical thermal analysis (DMTA) using a dynamic mechanical analyzer, Triton 2000 DMA (Triton Technology), under compression. Circular samples of 1 cm^2 and 3–4 mm thick were used. Samples were first cooled down to -100 ℃ with liquid nitrogen and heated to 100 ℃ at a heating rate of 4 ℃ min^{-1} and 1.0 Hz frequency during the measurement of the mechanical modulus.

Impedance spectroscopy. Electrochemical impedance spectroscopy (EIS) using an Autolab 302N potentiostat/galvanostat coupled to a Microcell HC temperature controller was undertaken to study the ionic conductivities. A circular Φ 11.28 mm membrane was sandwiched between two stainless steel electrodes and sealed in a microcell under an argon atmosphere. The measurements were carried out from 85 to 25 ℃ with a 30 min dwell time. The frequency range was from 0.1 MHz to 0.1 Hz and a 10 mV perturbation signal was applied. Ionic conductivities were calculated using the following equation[4]:

$$\sigma = \frac{1}{R_b} \cdot \frac{d}{S}$$

where σ is the ionic conductivity (S cm^{-1}), d is the thickness (cm) of the ionogels, S is the area of electrodes in contact with the GPE (cm^{-2}) and R_b (Ω) is the bulk resistance of the ionogel obtained from the Nyquist plot.

Lithium transference number (t_{Li^+}). The amount of ionic conductivity carried by the lithium ions was calculated using the following equation, as proposed by Evans, Vincent and Bruce[5]:

$$t_{Li^+} = \frac{I_s(\Delta V - I_0 \cdot R_0)}{I_0(\Delta V - I_s \cdot R_s)}$$

A DC bias (ΔV, 10 mV) was applied to polarize the polymer electrolytes during chronoamperometry, in which I_0 is the initial value of the current upon polarization and I_s is the current reached in the steady state. R_0 and R_s are the resistances of the solid electrolyte interphase, SEI, before and after the polarization, respectively, obtained by EIS.

Battery cell preparation

Electrodes. Negative electrodes: a circular thin foil of lithium metal (Φ 11.28 mm, 120 µm thick from Rockwood Lithium (US)) was deposited on top of a stainless steel electrode. Air-O_2 electrodes were prepared by coating a gas diffusion layer (GDL from Quintech (GER)) with a slurry containing Ketjen Black 600 carbon, LITHion^{TM} dispersion binder and anhydrous 2-propanol, as previously reported[6]. The coated GDLs had an average carbon loading of 0.72 mg cm^{-2}.

Symmetrical lithium cells. The UV-cured ionogels (Φ 11.28 mm) were sandwiched between two lithium foils (Φ 8 mm) and placed between two stainless steel spacers (Φ 11.28 mm) electronically isolated by a PEEK cylinder and tightened by three nut-bolt-insulator screws. A Teclock thickness gauge was used to ensure that the thickness of the electrolyte was even all along the electrode | electrolyte contact surface. Before testing, this assembly was placed in a sealed container to ensure an inert atmosphere.

Li-O_2 battery cells. Li-O_2 Swagelok cells were used and placed in a specifically designed PEEK container. The ionogels (Φ 11.28 mm) were sandwiched between the negative and positive electrodes and 75 µL of the liquid electrolyte was added as catholyte. In the case of liquid Li-O_2 cells, two glass fiber sheets, previously dried at 150 ℃ under vacuum for 24 h, (Φ 11.28 mm, Whatman®, GF/A grade) -soaked with the liquid electrolyte mixture (200 μL) were used. The positive electrode was placed with the coated side facing the electrolyte surface and an aluminum mesh was used as the current collector. Lithium metal (Φ 11.28 mm) was used as the negative electrode. This Swagelok cell was then transferred inside a sealed PEAK container, where the argon gas was purged and replaced by oxygen gas (Praxair, >99.5%).

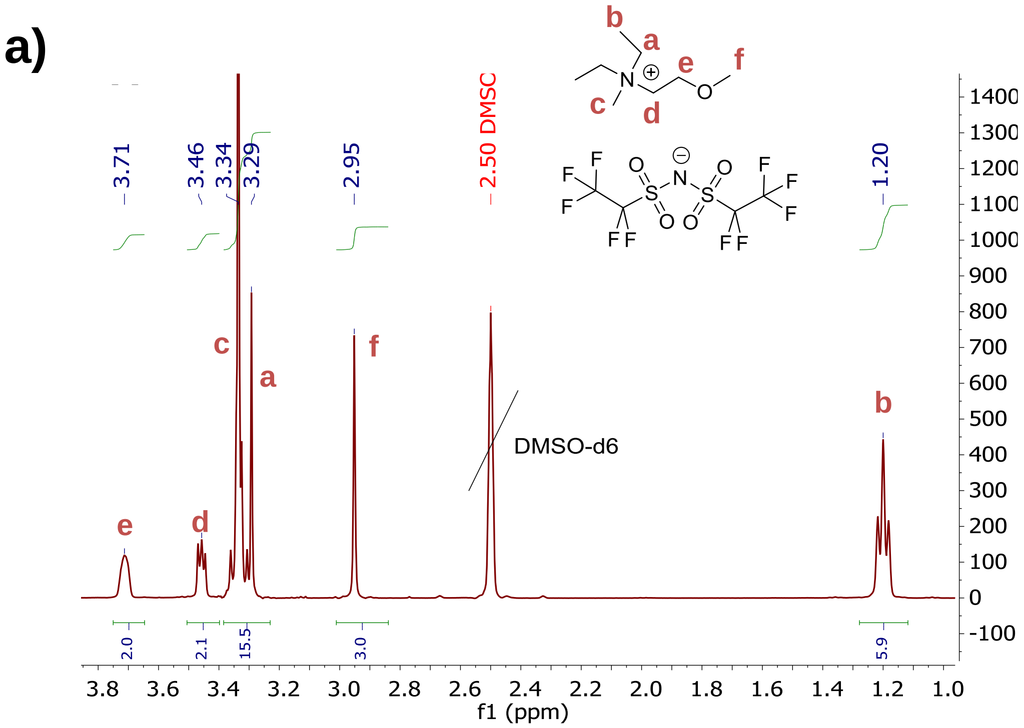
a)
3.71
3.46
3.34
3.29
2.95
2.50 DMSO
1.20
b
a
e
f
c
d
N
O
F
S
DMSO-d6
2.0
2.1
15.5
3.0
5.9
1400
1300
1200
1100
1000
900
800
700
600
500
400
300
200
100
0
-100
3.8
3.6
3.4
3.2
3.0
2.8
2.6
2.4
2.2
2.0
1.8
1.6
1.4
1.2
1.0
f1 (ppm)

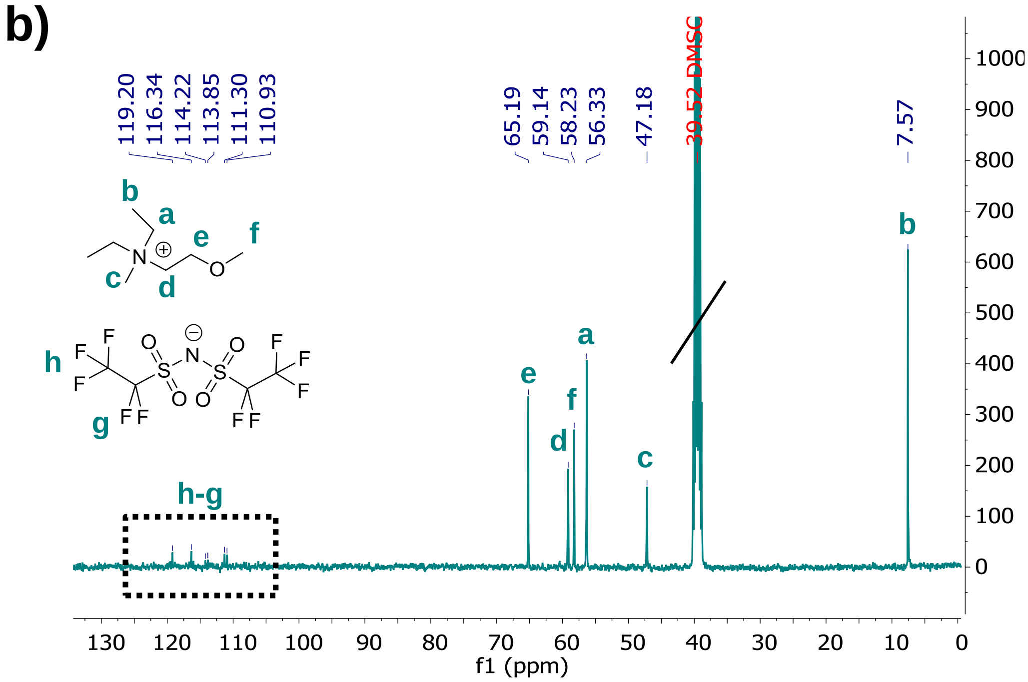
b)
119.20
116.34
114.22
113.85
111.30
110.93
65.19
59.14
58.23
56.33
47.18
39.52 DMSO
7.57
b
a
e
f
c
d
h
g
h-g
N
O
F
S
1000
900
800
700
600
500
400
300
200
100
0
130
120
110
100
90
80
70
60
50
40
30
20
10
0
f1 (ppm)

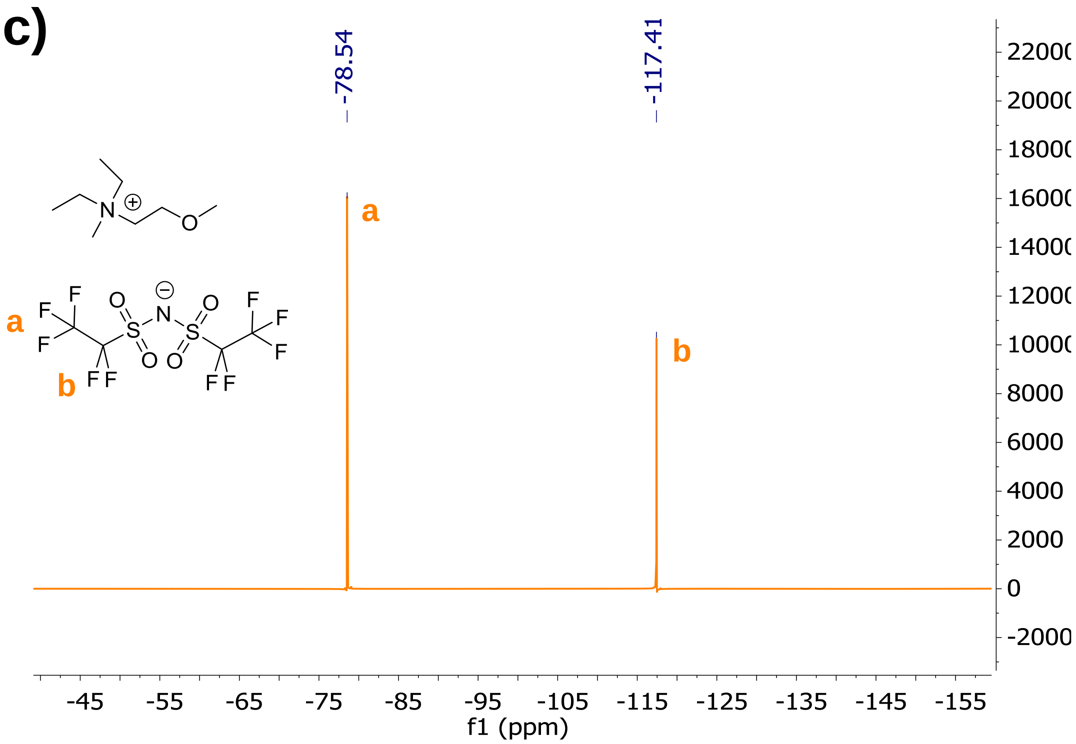

Figure S1. NMR spectra of DEME-BETI ionic liquid: a) ^{1}H NMR; b) ^{13}C NMR; c) ^{19}F NMR.

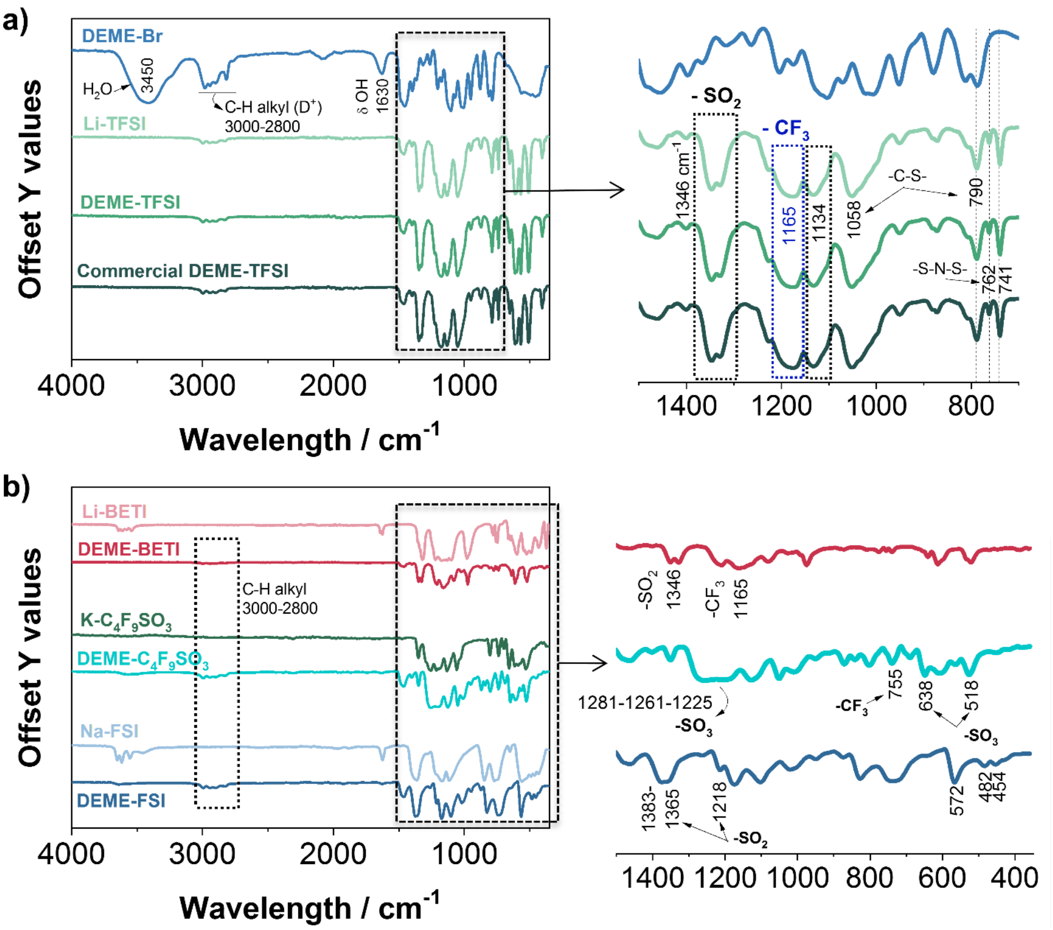

Figure S2. FTIR spectra of synthesized ionic liquids: a) DEME-TFSI ionic liquid compared to the synthesis precursors and the analog commercial product; b) DEME-BETI and DEME-CFSO and DEME-FSI ionic liquids.

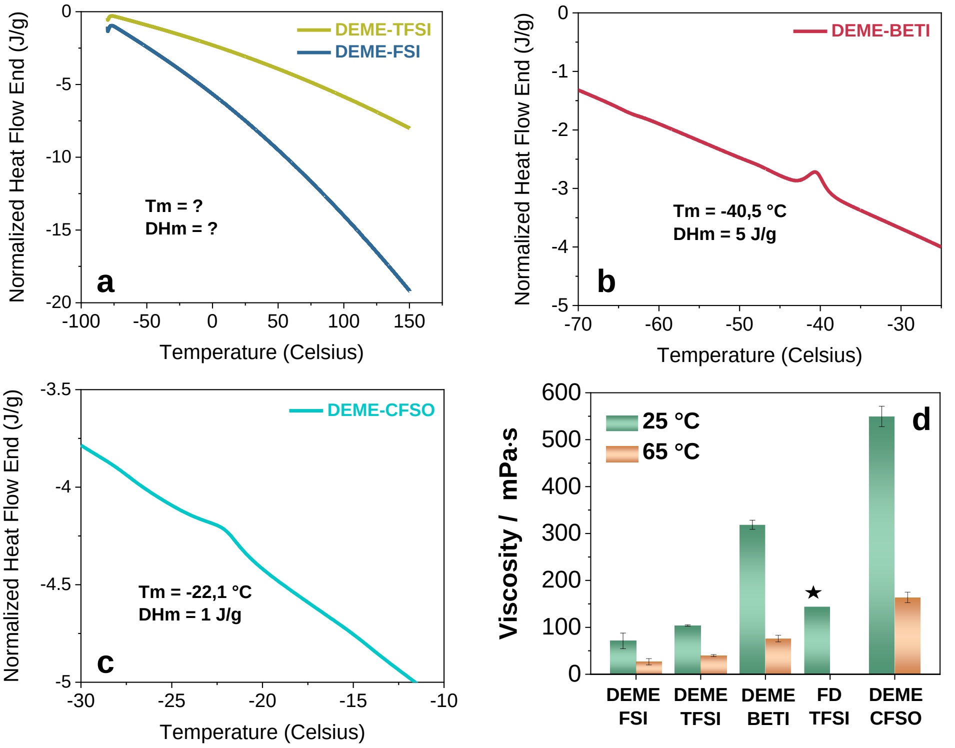

Figure S3. DSC thermograms of a) DEME-TFSI and DEME-FSI, b) DEME-BETI and c) DEME-CFSO ionic liquids. d) Dynamic viscosity of the ionic liquids measured at 25 and 60 ℃. Value of FD-TFSI at 25 °C (black "star") was found in the literature[1].

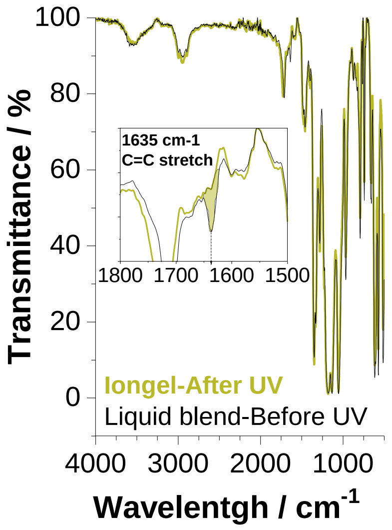

Figure S4. FTIR spectra of the Iongel-20 mol.% sample, based on DEME-TFSI, before (liquid blend) and after UV-photopolymerization. The 1635 cm^{-1} band, which is associated with the carbon double bond of acrylate functionalities[7], disappeared from the polymeric iongel.

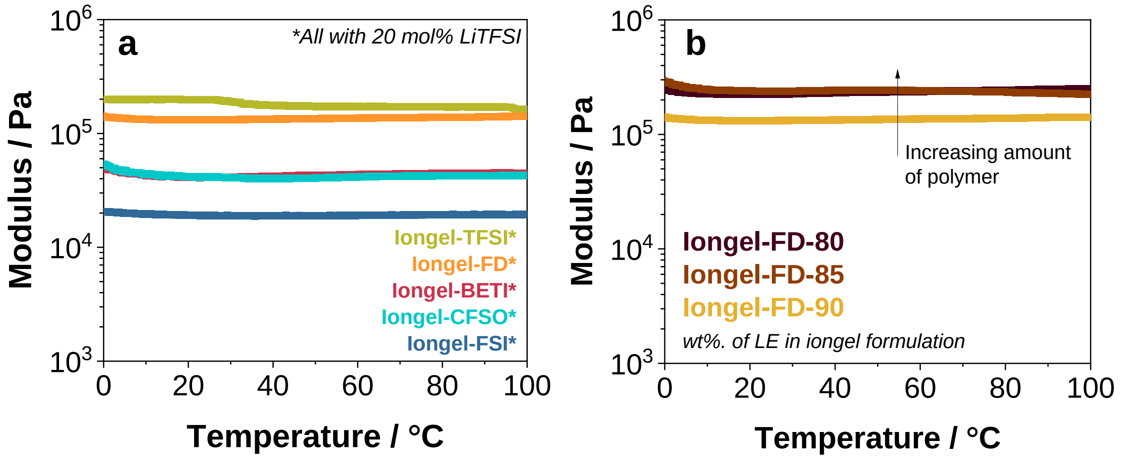

Figure S5. DMTA at compression from 0 to 100 ℃ of a) iongel membranes containing 20 mol.% of LiTFSI (Iongel-XX*) and b) iongel membranes based on FD-TFSI ionic liquid and containing 80, 85 and 90 wt.% liquid electrolytes.

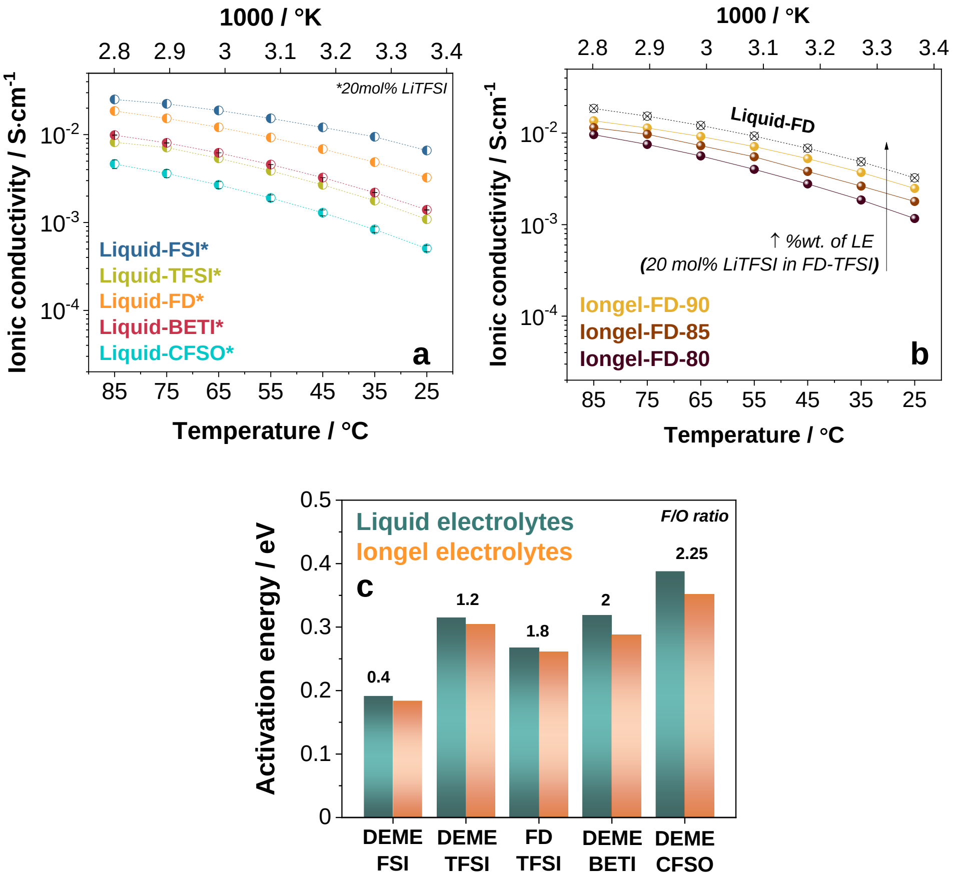

Figure S6. Ionic conductivity at different temperatures from EIS of a) liquid electrolytes containing 20 mol.% of LiTFSI (Liquid-XX*), b) Iongel-FD-XX electrolyte containing increasing amounts of liquid electrolyte, XX = 80, 85 and 90 wt.%. c) Activation energies calculated from Arrhenius equation[8,9].

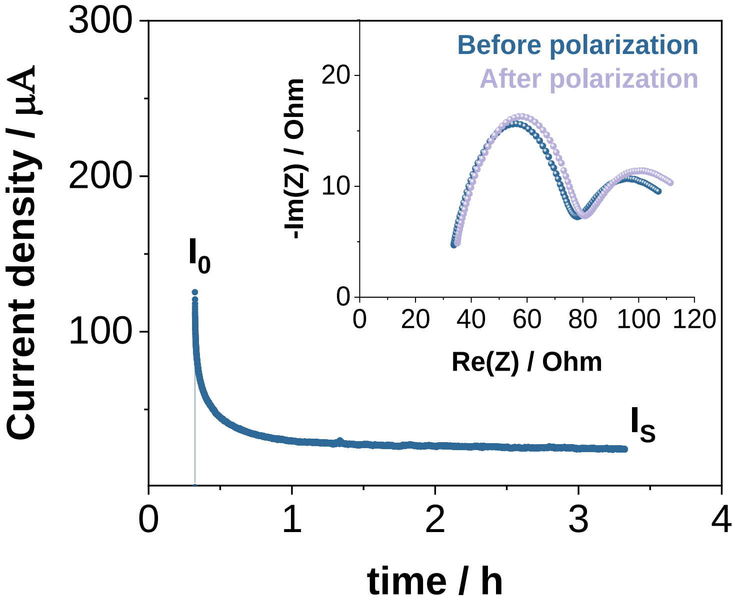

Figure S7. Chronoamperometry and EIS curves before and after polarization for lithium transference number calculation of cells containing Iongel-FSI electrolyte following the Evans–Vincent–Bruce method[5].

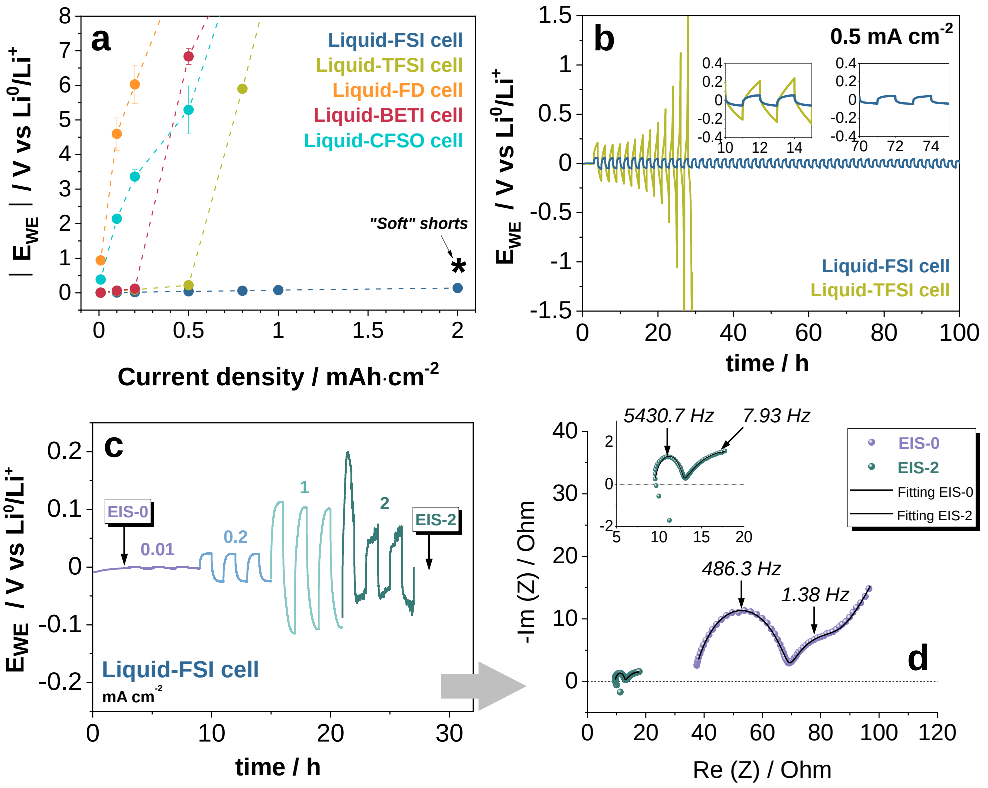

Figure S8. Tests on symmetrical lithium cells. a) Galvanostatic test with increasing current density from 0.01 to 2 mA cm^{-2} at 60 ℃. Plots show the average potentials achieved at each current density in cells containing ILEs. b) Long cycling at 0.5

mA cm^{-2} and 60 ℃ using Liquid-FSI and Liquid-TFSI liquid electrolytes. c) Lithium stripping/plating profiles of symmetrical lithium cells using Liquid-FSI electrolyte at increasing current rates and d) before and after cycling Nyquist plots.

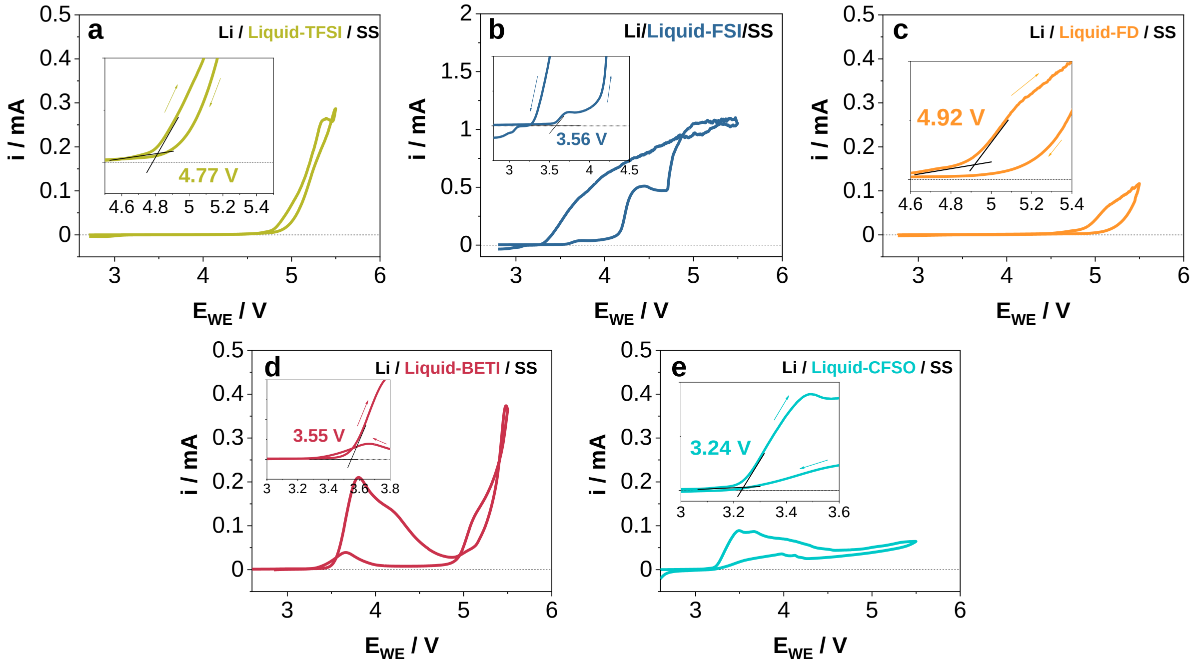

Figure S9. Voltammograms from OCV to 5.5 V at 60 ℃ at a scan rate of 0.2 mV s^{-1} for Li^{0}/electrolyte/stainless steel cells with ionic liquid-based electrolytes: a) Liquid-TFSI; b) Liquid-FD; c) Liquid-BETI; d) Liquid-CFSO; e) Liquid-FSI.

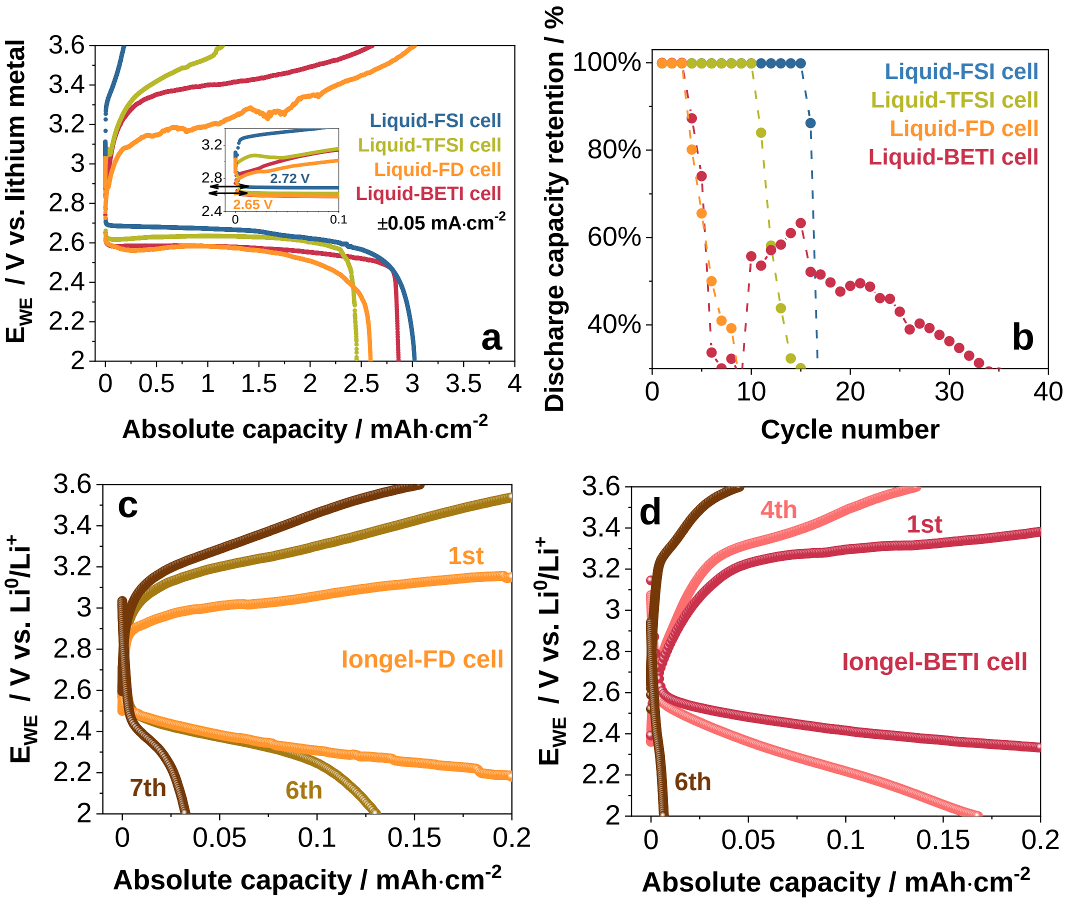

Figure S10. Swagelok Li-O_2 cells at 60 ℃. a) Discharge-charge profiles at 0.05 mA cm^{-2} of cells containing liquid electrolytes. b) Discharge capacity retention during cycling at a current of ±0.05 mA cm^{-2} with limited capacity (0.2 mAh cm^{-2}) of cells using liquid electrolytes. c) Selected potential profiles during cycling of cells using Iongel-FD. d) Selected potential profiles during cycling of cells using Iongel-BETI.

References

1. Vanhoutte G, Hojniak SD, Bardé F, Binnemans K, Fransaera J. Fluorine-functionalized ionic liquids with high oxygen solubility. *RSC Adv*. 2018;8(9):4525-4530. doi:10.1039/c7ra13403g

2. Gouveia ASL, Tomé LC, Lozinskaya EI, Shaplov AS, Vygodskii YS, Marrucho IM. Exploring the effect of fluorinated anions on the CO2/N2 separation of supported ionic liquid membranes. *Physical Chemistry Chemical Physics*. 2017;19(42):28876-28884. doi:10.1039/c7cp06297d

3. Costa AJL, Soromenho MRC, Shimizu K, et al. Density, thermal expansion and viscosity of cholinium-derived ionic liquids. *ChemPhysChem*. 2012;13(7):1902-1909. doi:10.1002/cphc.201100852

4. Qian X, Gu N, Cheng Z, Yang X, Wang E, Dong S. Methods to study the ionic conductivity of polymeric electrolytes using a.c. impedance spectroscopy. *Journal of Solid State Electrochemistry*. 2001;6(1):8-15. doi:10.1007/s100080000190

5. Zugmann S, Fleischmann M, Amereller M, Gschwind RM, Wiemhöfer HD, Gores HJ. Measurement of transference numbers for lithium ion electrolytes via four different methods, a comparative study. *Electrochim Acta*. 2011;56(11):3926-3933. doi:10.1016/j.electacta.2011.02.025

6. Alvarez-Tirado M, Castro L, Guzmán-González G, Porcarelli L, Mecerreyes D. Single- Versus Dual-Ion UV-Cross-Linked Gel Polymer Electrolytes for Li-O2 Batteries. *ACS Appl Energy Mater*. 2021;4:295-302. doi:10.1021/acsaem.0c02255

7. Vijayakumar V, Anothumakkool B, Kurungot S, Winter M, Nair JR. In Situ Polymerization Process: An Essential Design Tool for Lithium Polymer Batteries. *Energy Environ Sci*. 2021;14:2708-2788. doi:10.1039/d0ee03527k

8. Aziz SB, Woo TJ, Kadir MFZ, Ahmed HM. A conceptual review on polymer electrolytes and ion transport models. *Journal of Science: Advanced Materials and Devices*. 2018;3(1):1-17. doi:10.1016/j.jsamd.2018.01.002

9. Singh VK, Shalu, Balo L, Gupta H, Singh SK, Singh RK. Solid polymer electrolytes based on Li+/ionic liquid for lithium secondary batteries. *Journal of Solid State Electrochemistry*. 2017;21(6):1713-1723. doi:10.1007/s10008-017-3529-z